

Research and calibration of Acoustic Sensors in ice within the SPATS (South Pole Acoustic Test Setup) project

Thomas Meures^a, Larissa Paul^a, Mathieu Ribordy^b, for the IceCube collaboration^c

^a*III Physikalisches Institut, RWTH Aachen University, D-52064 Aachen, Germany*

^b*Laboratory for High Energy Physics, École Polytechnique Fédérale, CH-1015 Lausanne, Switzerland*

^c*http://icecube.wisc.edu*

Abstract

We present development work aiming towards a large scale ice-based hybrid detector including acoustic sensors for the detection of neutrinos in the GZK range. A facility for characterization and calibration of acoustic sensors in clear (bubble-free) ice has been developed and the first measurements done at this facility are presented. Further, a resonant sensor intended primarily for characterization of the ambient noise in the ice at the South Pole has been developed and some data from its performance are given.

Keywords: Acoustic neutrino detection, SPATS

1. Introduction

An important supplement to the in situ test at South Pole with the South Pole Acoustic Test Setup (SPATS) [1] are the laboratory activities at all contributing institutions. We describe here first the facility for measurements on sensors and transmitters frozen into a 3 m³ high quality ice-block. The facility will also be used for measurements with thermo-acoustically generated pulses, but this will not be described below. We further describe a resonant sensor that has been developed primarily for determination of the ambient noise level in the ice at the South Pole. It may also be a possible sensor in a complementary part of a radio array intended for detection of GZK neutrinos at the South Pole.

2. The Aachen Acoustic Laboratory

2.1. AAL facility

In the Aachen Acoustic Laboratory (AAL), an Ice-Top tank has been set up inside a cooling container for calibration of acoustic sensors in ice. In the cylindrical tank, with a diameter of 190 cm and a used height of 85 cm, bubble-free ice can be produced with the help of a freeze control unit (FCU) [2]. The FCU is equipped with a vacuum pump connected to a semi-permeable membrane, in order to degas the water. The water in the tank freezes starting from the top. To take out the surplus water under the ice, an overflow reservoir is used.

The total freezing of the 3 m³ of water takes around 70 days.

Inside the tank, 18 piezo-based sender/sensor-pairs are mounted on a dodecagonal aluminum frame embedded in the ice volume. Each of the three levels holds six sender/sensor pairs in a hexagon structure. The levels are located at 5 cm, 25 cm, and 45 cm below the ice surface. The third level is situated 40 cm above the bottom of the tank. The used senders and sensors are simple Piezoelectric Transducer (PZT) discs in an aluminum housing produced by Murata [5]. The sensors are equipped with a pre-amplifier with a gain of 100 and a differential output. They are calibrated absolutely by means of the reciprocity method and serve as reference for calibration of other acoustic devices. The accuracy of the positioning system was checked during the freezing using a χ^2 minimization of the arrival times of acoustic signals produced by the senders [4]. The positions were reconstructed with an accuracy of 0.5 cm.

2.2. Reciprocity calibration in the AAL

The sensors, used in the AAL setup as calibration references, are themselves calibrated by means of the reciprocity method [3]. This method is based on the reciprocity principle, developed for systems such as electro-acoustic converters. It leads to the reciprocity equation:

$$M = JS. \quad (1)$$

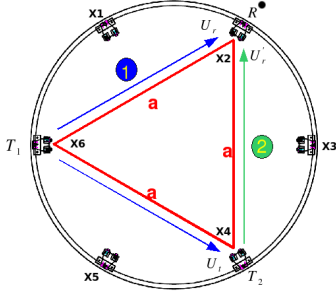


Figure 1: A schematic setup for the calibration of one sensor R with two transmitters T_1 and T_2 .

Here, $M = U/p$ is the sensitivity of the converter. It is the ratio of a response voltage U at the sensor and the incident pressure p , causing the sensor response. The emissivity $S = p_0/I$ is the ratio of an emitted pressure at a distance of one meter and the applied current to the converter [6]. The reciprocity coefficient J has to be determined individually for each sensor type. We calculated J by using the baffled piston model [6]. The coefficient is:

$$J = \frac{2\pi r}{\omega \rho_0} \cdot \frac{1}{\lambda_T(\alpha, \omega)} \quad (2)$$

Here r is the distance between the sender and the sensor, ω the angular frequency of a signal, ρ_0 the density of the medium and $\lambda_T(\alpha, \omega)$ the angular dependence of the converter sensitivity and emissivity for the angle α and angular frequency ω .

The sensors are mounted in the corners of a hexagon, such that an equilateral triangle is formed by three sensors. For the reciprocity calibration of a sensor R (Fig. 1) a transmitter T_1 on one corner of the triangle transmits to the sensor and the second sensor/transmitter T_2 with a broad band signal. Being at the same distance both sensors receive the same sound field. The output voltages U_R and U_T are recorded. Subsequently, a current I is applied to the reference transmitter T_2 which causes an acoustic signal to be sent, recorded by R and resulting in an output voltage U'_R . The sensitivity can then be determined by

$$M_R = \frac{1}{\lambda_R(\alpha, \omega)} \cdot \sqrt{\frac{U_R U'_R 2\pi r}{U_T I_T \omega \rho_0}} \quad (3)$$

Here λ_R the angular dependence of the sensor. To calculate the current I , applied to the reference transmitter, its impedance has to be measured. For an electro-acoustic converter an electric analog can be set up. In

the case of a piezo-element it is a capacitance with RCL-circuits in parallel, each representing a resonance of the sensor.

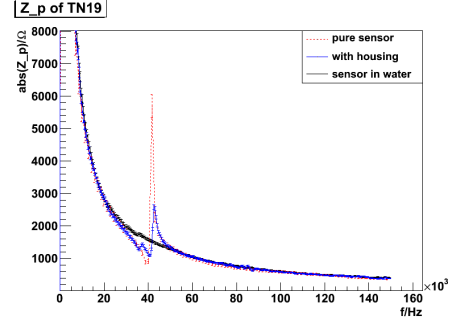


Figure 2: The comparison of the impedance in air and water, showing the reduced resonance in water. "Pure sensor" indicates the status as delivered by Murata. The "Housing" is added in the AAL for the fixing on the positioning system.

In the case of the Murata sensors in water and ice, the representation is reduced to a simple capacitor due to the reduced resonances, see Fig. 2 for water. Results for the sensors in water and ice are shown in Fig. 3 and in Fig. 4.

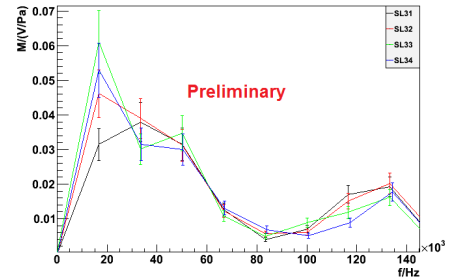


Figure 3: The sensitivity of the four sensors at level 3 in water.

For the calibration in ice an extra sender is needed, to get a strong input signal at low frequencies. For this reason an underwater loudspeaker is used, installed in the middle at the bottom of the IceTop-tank. This loudspeaker is designed for high emission power at low frequencies ($f < 30$ kHz).

The systematic errors of the measurements are calculated individually for each sender to 15% and for each sensor to 13%. The global error on the calibration measurements is 5% for the senders and 11% for the sensors. The uncertainties are dominated by three components: the error on the angular dependence of the sensitivity and emissivity, the error on the capacitance

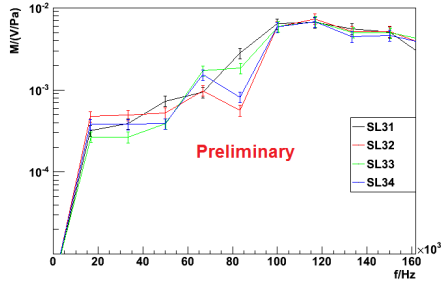


Figure 4: The sensitivity of the four sensors in level 3 in ice.

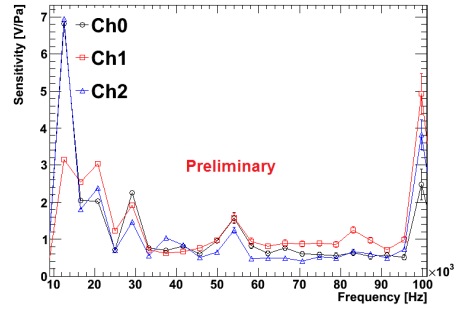


Figure 5: Sensitivity for the three channels of the SPATS sensor in water.

103 of the piezo and the error on the reciprocity factor [8].
 104 The last one will be reduced in a future setup by including
 105 senders following a different reciprocity model with
 106 less systematic dependencies. The error on the sender
 107 impedance can be reduced by a factor of two, by using
 108 an upgraded type of sender. The error on the angular
 109 dependence can be reduced by measuring a frequency-
 110 dependent angular factor for each sensor individually
 111 [10]. This, especially in ice, is complicated, but will
 112 be done for the required angles in future measurements.
 113 These systematic errors are dominant for the calibration
 114 apart from the in ice calibration of the senders. The low
 115 power of the senders in ice leads to statistical uncertain-
 116 ties of about 50% [8].

117 2.3. Calibration of a SPATS sensor

118 The SPATS sensor was developed for the South Pole
 119 Acoustic Test Setup [1] deployed at South Pole. It consists
 120 of three piezo elements pressed against the inner steel
 121 housing, a cylinder with a diameter of 10.1 cm. For readout
 122 the voltage produced by the piezos is amplified, and sent
 123 to a highpass filter ($f > 5$ kHz) and a lowpass filter
 124 ($f < 100$ kHz). The SPATS sensor was installed at an
 125 ice depth of 45 cm directly in the center of the tank.
 126 The sensitivity of the SPATS sensor is calculated using
 127 $M = U/p$. The pressure is calculated using the known
 128 sensitivity of the AAL sender. It is given by:

$$129 \quad p = \frac{S_t I}{d} = \frac{M_t I}{Jd} \quad (4)$$

130 The sensitivities for one SPATS sensor in water are
 131 shown in Fig. 5. The calibration measurement in water
 132 is consistent with the results in [7]. The systematic
 133 errors are 23%. They are dominated by the error of the
 134 senders sensitivities in Sec. 2.2. The peaks in the spec-
 135 trum at low frequencies arise from resonances of the
 136 steel housing and are not related to the intrinsic piezo
 137 resonances.

We observe a strong reduction of the sensitivity from

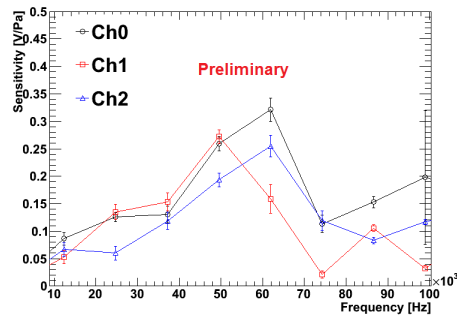


Figure 6: Sensitivity for the three channels of the SPATS sensor in ice.

138 water to ice for all frequencies < 100 kHz, shown in Fig.
 139 6. This result has not been confirmed in an independent
 140 measurement yet. A problem for the in-ice calibration
 141 is the extremely low emissivity of the Murata senders
 142 in ice, which results in large systematic uncertainties of
 143 56% [9]. The loudspeaker could not be used for the
 144 measurements reported here, since it is positioned di-
 145 rectly beneath the SPATS sensor. It is planned to redo
 146 the measurement with improved senders, which have a
 147 higher emissivity.

148 3. Resonant Sensor

149 A multi-channel acoustic PZT-based sensor encased
 150 in a stainless steel housing was recently developed at
 151 École Polytechnique Fédérale de Lausanne (EPFL). The
 152 overall design is similar to the design of the sensors
 153 used by SPATS [1]. Immersed in water, the sensor housing
 154 exhibits strong resonant behavior at a fundamental fre-
 155 quency of about 23 kHz. In an ice environment with
 156 higher speed of sound however, one expects the reso-
 157 nance to be damped due to a closer impedance match
 158 with the surrounding medium. The sensor dimensions
 159 were chosen to match well the expected main frequency
 160 content of an acoustic pulse generated by an UHE neu-

161 trino in ice [11, 12]. This sensor is not likely to perform
 162 as well as a sensor with a flat frequency response curve
 163 for the characterization of the exact frequency content
 164 of a short transient excitation. On the other hand, the
 165 rather sharp frequency response allows to reduce the
 166 bandwidth in the PZT amplifiers, thereby decreasing
 167 electrical noise.

168 Two versions of the resonant sensor exist, with digital or
 169 analog transmission lines. The digital version has two
 170 parallel 8 MHz digital transmission lines which have
 171 now been successfully tested over 500 m ethernet cables
 172 (each transmission line carries the multiplexed signal of
 173 two sensor channels and a 12-bit digitizer samples each
 174 channel signal at the rate of 250 MSPS). More details
 175 on the sensor layout, components and electronics can
 176 be found in [13], as well as a discussion of its pointing
 177 capabilities (with the sensor encased in an aluminium
 178 housing instead).

179 Fig. 7 shows the frequency response of one of the sensor
 180 channels to a 30 mPa signal (single sine period, 20
 181 kHz) and for comparison the noise from a single 8.192
 182 ms data acquisition sample in open water. Fig. 8 shows
 183 the self noise of the sensor at frequencies between 10
 184 and 60 kHz.

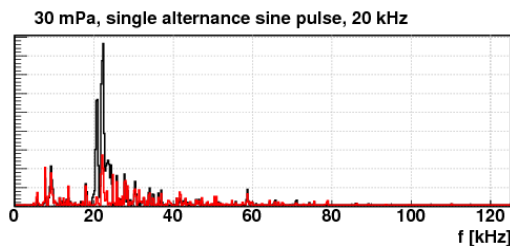


Figure 7: Sensor response (power spectrum squared) to a 30 mPa pulse (20 kHz single sine period). Typical noise in red.

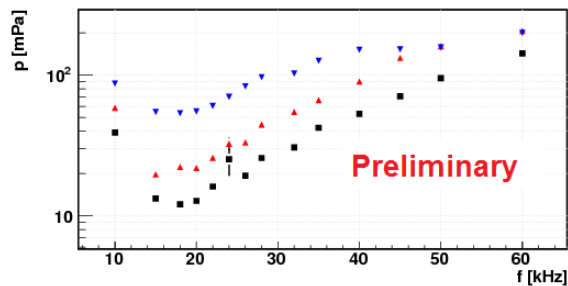


Figure 8: Equivalent pressure of the self noise w.r.t. the frequency of a single sine period excitation pulse for three channels.

185 4. Outlook

186 The activities for acoustic neutrino detection at the
 187 South Pole continue. Sensors from EPFL and modified
 188 SPATS sensors, supplemented with a floating PZT
 189 emitter in their center for absolute calibration are currently
 190 undergoing intensive testing (including freezing tests
 191 and calibration in ice) at the AAL facility. In the
 192 context of the continued SPATS project aiming for the
 193 absolute acoustic noise level measurement we anticipate
 194 the deployment of additional sensors at the South Pole
 195 this winter.

196 References

- 197 [1] S. Boeser *et al.*, Int. J. Mod. Phys. A **21S1** (2006) 107.
 198 [2] T. Stanev and the IceCube Collaboration, "Status, performance,
 199 and First results of the IceTop array", Nuclear
 200 Physics B - Proceedings Supplements 196, 159-164 (2009),
 201 arXiv:0903.0576v1.
 202 [3] R. J. Urick, "Principles of underwater sound", 3rd ed., Peninsula
 203 Publishing (1983).
 204 [4] S. Zierke, bachelor thesis, RWTH Aachen (2010)
 205 [5] Murata Manufacturing Co., Ltd., "Piezoelectric Ceramics
 206 (PIEZOTITE) Sensors", *Cat.No.P19E-9*, Japan(2008)
 207 [6] R.Lerch, G.M. Sessler, D. Wolf, "Technische Akustik: Grundlagen
 208 und Anwendungen", Springer-Verlag, Berlin (2009)
 209 [7] J.H.Fischer, "Acoustic transducers for the South Pole Acoustic
 210 Test Setup", diploma thesis, Humboldt University Berlin (2006)
 211 [8] T. Meures, diploma thesis, RWTH Aachen (2010), IceCube Internal
 212 Reports "icecube/201010002"
 213 [9] L. Paul, diploma thesis, RWTH Aachen (2010), IceCube Internal
 214 Reports "icecube/201010001"
 215 [10] B. Semburg, phd thesis, University of Wuppertal, to be published
 216 [11] J.G. Learned, Phys. Rev. 19 (1979) 3293.
 217 [12] S. Bevan *et al.*, Astropart. Phys. 28 (2007) 366.
 218 [13] M. Podgorski and M. Ribordy, proc. of the 31st ICRC, July
 219 2009, Lodz, Poland.
 220